EWEA 2015 Annual Event - Abstract

Abstract title: Aerodynamic analysis of 10 MW-class wind turbine using CFD

Ryo Yamada*, Keiichi Murakami, Atsushi Hashimoto, Takashi Aoyama, Yuichi Matsuo, Chuichi Arakawa, Makoto Iida**

Ryo Yamada, Chuichi Arakawa and Makoto Iida, The University of Tokyo, 7-3-1 Hongo, Bunkyo-ku, Tokyo, Japan

Keiichi Murakami, Atsushi Hashimoto, Takashi Aoyama, Yuichi Matsuo, Japan Aerospace Exploration Agency, 7-44-1 Jindaijihigashimachi, Chofu-shi, Tokyo, Japan

Key Words: 10 MW-class Wind Turbine, CFD, BEM, Two-Bladed Wind Turbine

1. Introduction

Wind turbine rotor diameters have been upsized to increase the power and utilize higher wind speeds for decreased power costs[1]. Today, investigations for the realization of wind turbines with a rated power output of 10 MW are being undertaken[2][3]. When upsizing the diameter, increased blade mass and manufacturing costs are not negligible. Thus, some solutions to these problems are suggested as follows: change the blade structure or material[2][4] and reduce the number of blades by applying two-bladed rotors[3][5]. In particular, the application of two-bladed rotors is a good solution because it can reduce both rotor mass and manufacturing costs.

However, there are some problems with two-bladed rotors. For example, because they are inferior to three-bladed rotors in aerodynamic balance, they are more sensitive to yaw error and the atmospheric boundary layer (ABL). Furthermore, aerodynamic loads on the blades increase for two-bladed rotors. Thus, to apply a two-bladed rotor to a 10 MW-class wind turbine, it is necessary to investigate the effects of reducing the number of blades on aerodynamic characteristics. Considering the Reynolds number effect, it is desirable to perform these investigations on actual-scale wind turbine. However, it is impossible to implement the experiments using actual wind turbines. On the other hand, a computational fluid dynamics (CFD) analysis of actual wind turbines is possible. Furthermore, more detailed information about the flow structure around the blade can be obtained by CFD. Thus, it is worth evaluating the effects of applying a two-bladed rotor to a 10 MW-class wind turbine by CFD. Furthermore, there are few studies focused on these problems.

The goal of this project is to contribute to the development of a 10 MW-class wind turbine by clarifying the aerodynamic characteristics of two- and three-bladed rotors in the ABL and with yaw error, which affects aerodynamic balance. In this study, we execute the CFD analysis under uniform inflow conditions for the purpose of the validation and confirmation of rotor performance through comparison with the blade element momentum (BEM) theory result. Next, we compare the difference between aerodynamic characteristics in two- and three-bladed rotors.

*Presenting author. ** Corresponding author.
E-mail: r.yamada@gg.cfdl.t.u-tokyo.ac.jp (Ryo Yamada),
iida@ilab.eco.rcast.u-tokyo.ac.jp (Makoto Iida)

2. Approach

2-1. Analysis objective

We selected NEDO 10 MW RWT[3], which was proposed as the reference 10 MW-class offshore wind turbine in Japan by the New Energy and Industrial Technology Development Organization (NEDO). The specifications for NEDO 10 MW RWT are shown in Table 1. Two- and three-bladed rotor models are proposed. The three-bladed model used in the CFD analysis is shown (without nacelle or spinner) in Fig. 1.

Table 1. Specifications for NEDO 10 MW RWT.

	Two-bladed	Three-bladed
Rotor position [-]	Upwind	
Rotor diameter [m]	200	
Number of blade [-]	2	3
Rated tip speed[m/s]	110	90
Rated tip speed ratio [-]	12.2	10
Rated number of revolution [rpm]	10.5	8.6
Airfoil profiles [-]	FFA-W3	

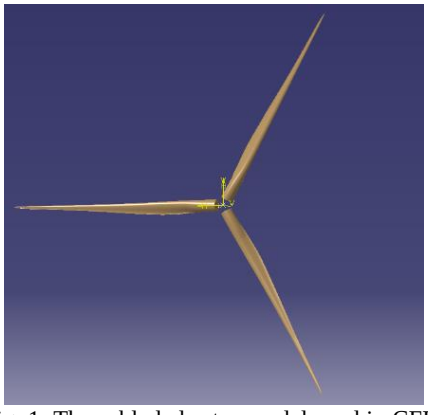

Fig. 1. Three-bladed rotor model used in CFD.

2-2. Analysis code

In this study, we used the fast CFD solver FaST Aerodynamic Routines (FaSTAR)[6] developed by the Japan Aerospace eXploration Agency (JAXA) for executing low cost CFD analyses[7]. The governing equations are the compressible Navier-Stokes equations, which are discretized using a finite volume method (FVM). FaSTAR is an unstructured grid flow solver, so it is used with HexaGrid[8][9], developed by JAXA for generating unstructured grids automatically, so fast CFD analysis is enabled.

2-3. Computational grid

Grid information from this study is shown in Table 2. Computational grids are generated by HexaGrid; the grid near the blade is prismatic and the one for the far-field region is Cartesian. Denoting the rotor diameter as D, the analysis domain is $10D \times 10D \times 10D$, and the rotor is set at the center of the domain. We set the "refinement region" as 1D downstream from the rotor plane, where the grid resolution is subdivided so that the resolution around the blade is sufficiently small. Denoting the chord length at $r/R = 0.8$ as c, the grid resolution on the blade is $0.022c$. Here R is the rotor radius. The height of the first cell on the blade is within $y^+ = 1$. The total number of cells is about 80 M in the three-bladed case and 52 M in the two-bladed case. The computational grid around the blade is shown Fig. 2, and the grid around the airfoil at $r/R = 0.8$ is shown in Fig. 3.

Table 2. Computational grid information.

Analysis domain	$10D \times 10D \times 10D$
Refinement region	$1.5D \times 1.5D \times 1.5D$
Resolution in refinement region	$1.6c \times 1.6c \times 1.6c$
Resolution on the blade	$0.022c$
Height of the first cell on the blade	$y^+ \approx 1$
Total number of cells	52 M (two-bladed) 80 M (three-bladed)
Remarks	$D = 200$ m $c = 1.9$ m (at *r/R*=0.8)

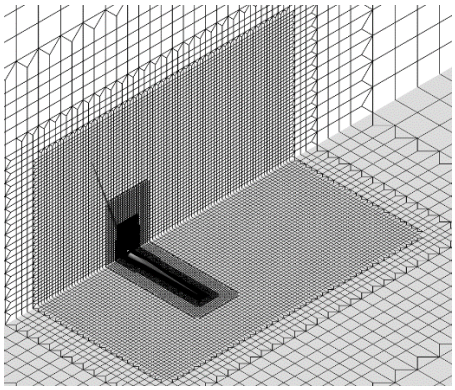

Fig. 2. Computational grid around the three-bladed rotor.

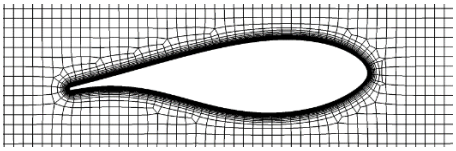

Fig. 3. Computational grid around the airfoil at $r/R = 0.8$.

2-4. Numerical analysis condition

In this study, numerical analysis conditions are shown in Table 3. We use the u-MUSCL scheme as the reconstruction method. Thus, the resolution in space is third-order for the uniform grid. The Spalart–Allmaras turbulence model is used as the turbulence model. The rotation of the rotor is represented by moving grids[10]. The analysis cases in this study are shown in Table 4. The tip speed is constant, and the inflow speed is changed for changing tip speed ratio λ. The blade pitch angle is constant, whereas the power coefficient is maximum at the rated λ.

Table 3. Numerical analysis condition.

Governing equations	Reynolds-averaged Navier-Stokes equations
Space discretization	Cell-centered FVM
Inviscid flux	SLAU
Gradient	GLSQ
Limiter	Hishida's limiter
Reconstruction	u-MUSCL
Turbulence model	Spalart-Allmaras
Rotation of wind turbine	Moving Grids
Time integration	LU-SGS
CFL number	1 (local time stepping)

Table 4. Analysis cases.

	Tip speed ratio λ [-]	Tip speed [m/s]
Two-bladed	4, 5, 6, 7, 8.3, 9, 10, 11, 12	90
Three-bladed	5, 6, 7, 8, 9, 10.1, 11, 12.2, 13	110

3. Main body of abstract

In this study, all computations were executed on JAXA Supercomputer Systems[11] (JSS), and the calculation time for each case was about 24 hours. The vorticity contour around the three-bladed rotor at $\lambda = 10$ is shown in Fig. 4 as an example of the obtained results. The flow field around the rotor was captured in this image.

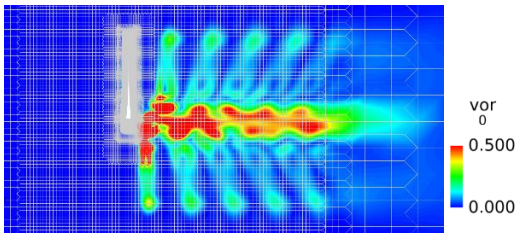

Fig. 4. Vorticity contour of three-bladed rotor at $\lambda = 10$.

3-1. Global Power/Thrust coefficients

The relationships between the global power/thrust coefficients C_P/C_T obtained by FaSTAR and the tip speed ratio λ are shown in Figs. 5 and 6, respectively. Moreover, the coefficients obtained by the BEM theory are also plotted. C_P and C_T can be calculated as (1) and (2), respectively:

$$C_P = \frac{P}{\frac{1}{2}\rho\pi U_\infty^3 R^2} \quad (1)$$

$$C_T = \frac{T}{\frac{1}{2}\rho\pi U_\infty^2 R^2} \quad (2)$$

Here P and T is power and thrust of the rotor, ρ is the density of inflow, U_∞ is the inflow velocity, respectively.

As shown in Fig. 5, the C_P values obtained by FaSTAR are consistent with those obtained by the BEM theory. As shown in Fig. 6, the C_T values obtained by FaSTAR are larger than those obtained by the BEM theory, but the trend with changing λ is correctly captured. Focusing on the difference in the number of blades, C_T of the two-bladed rotor changes more gradually than that of three-bladed rotor, which is consistent with general

wind turbines characteristics. Also, at the same inflow speed ($\lambda = 10$ for the two-bladed rotor and $\lambda = 12.2$ for the three-bladed rotor), C_T is the same, which shows the thrust per blade of the two-bladed rotor is larger than that of the three-bladed rotor.

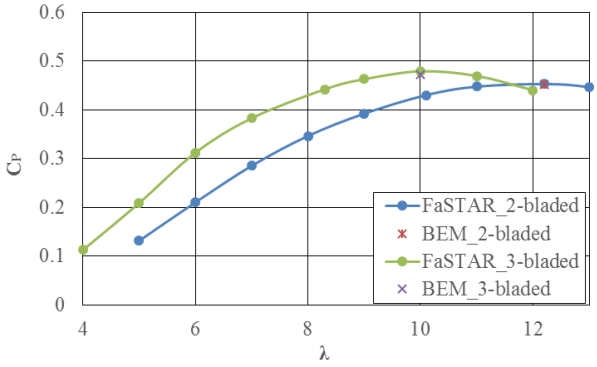

Fig. 5. Global power coefficient.

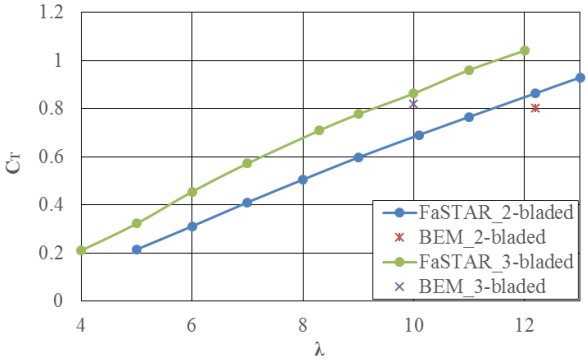

Fig. 6. Global thrust coefficient.

3-2. Local force distributions along the blade

Next, we focus on the local force distributions along the blade. Local force F_x acting in the normal direction of the rotor plane is shown in Fig. 8, and F_y acting in the tangential direction is shown in Fig. 9. Here F_x and F_y are defined as shown in Fig. 7.

As shown in Figs. 8 and 9, local forces obtained by FaSTAR are generally larger than those obtained by the BEM theory, but the trends show good agreement. Also, declines in the results obtained by FaSTAR at around $r/R = 0.15,\ 1.0$ are not seen in the BEM result. The declines around $r/R = 0.15$ are considered to be caused by three-dimensional flows induced by the transition of blade shape from cylinder to airfoil, and those around $r/R = 1.0$ are considered to be caused by tip losses. Thus, it is believed that CFD analysis can capture both tip losses and 3D effects, which are difficult to capture using the BEM theory.

When focusing on the difference in the number of blades, F_x of the two-bladed rotor and the rate of variability are larger than those of three-bladed rotor. Furthermore, complex fluctuations of F_x near the blade root are seen only in the case of the two-bladed rotor. Besides, F_y of the two-bladed rotor is negative at around $r/R = 0.15$, which is not seen in the case of three-bladed rotor. These phenomena suggest that tip losses and 3D effects are larger in two-bladed rotors than in three-bladed rotors.

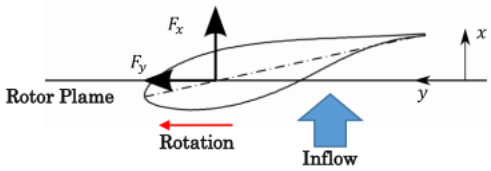

Fig. 7. Definition of local forces F_x and F_y along the blade.

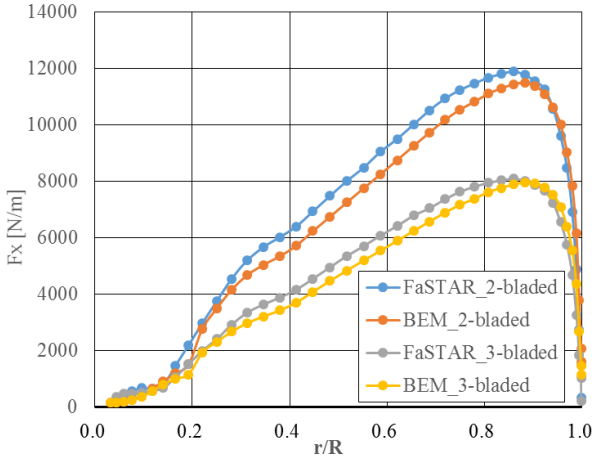

Fig. 8. Normal force F_x distributions along the blade.

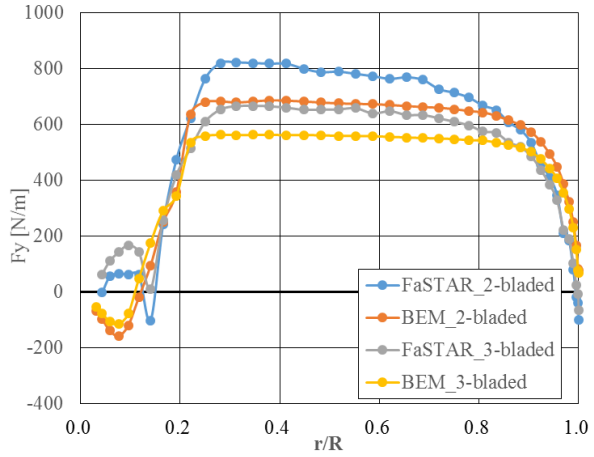

Fig. 9. Tangential force F_y distributions along the blade.

4. Conclusion

We executed a CFD analysis of two- and three-bladed rotors using a 10 MW-class offshore wind turbine proposed by NEDO as a reference. We implemented validations and verifications of rotor performance through comparison with the BEM result. Next, we investigated the difference in aerodynamic characteristics when changing the number of blades. The obtained results are as follows:

・The results obtained by CFD are generally consistent with the BEM theory results. Thus, wind turbine performance can be captured correctly in this study.

・It is believed that the CFD analysis executed in this study captured tip losses and 3D effects that are difficult to captured using the BEM theory.

・The tip losses and 3D effects are larger in two-bladed rotors than in three-bladed rotors.

5. Learning objectives

In this study, we focused on the aerodynamic characteristics of uniform inflow and investigated local force distributions along the blade, in detail, at the rated tip speed ratio. Next, we will focus on the differences in aerodynamic characteristics when the inflow speed changes. We will then execute a CFD analysis in the ABL and with yaw error to assess the difference in aerodynamic characteristics for two- and three-bladed rotors.

Acknowledgments

This study was supported by the NEDO project. In addition, we used the computational resources of JAXA.

References

[1] Technology Roadmap:Wind Energy-2013 edition, IEA

[2] Bak, Christian, *et al*. "The DTU 10-MW reference wind turbine." *Danish wind power research* (2013).

[3] “Research Study about 10-MW class wind turbine”, NEDO http://www.nedo.go.jp/content/100575922.pdf (2015/05/08 accessed)

[4] Bak, Christian, *et al*. "Light Rotor: The 10-MW reference wind turbine." *EWEA 2012-European Wind Energy Conference & Exhibition*. 2012.

[5] Bergami, Leonardo, Helge A. Madsen, and Flemming Rasmussen. "A Two-Bladed Teetering Hub configuration for the DTU 10 MW RWT: loads considerations." *European Wind Energy Conference & Exhibition 2014*.

[6] Hashimoto, Atsushi, *et al*. "Toward the fastest unstructured CFD code ‘FaSTAR’." *AIAA paper* 1075 (2012).

[7] Hashimoto, A., K. Murakami, and T. Aoyama. "JAXA Digital/Analog Hybrid Wind Tunnel: Decelopment of Digital Wind Tunnel." *Proceedings of the 2nd Workshop on Integration of EFD and CFD*. 2010.

[8] Hashimoto, Atsushi, *et al*. "Lift and Drag Prediction Using Automatic Hexahedra Grid Generation Method." *AIAA paper* 1365 (2009): 2009.

[9] Hashimoto, Atsushi, *et al*. "Drag Prediction on NASA CRM Using Automatic Hexahedra Grid Generation Method." *AIAA paper* 1417 (2010): 2010.

[10] J.Blazek, “Computational Fluid Dynamics: Principles and Applications, Second Edition,” Elservier, 2005.

[11] Inari, V. Takayuki Abe V. Tomohide, and V. Ken Seki. "JAXA Supercomputer Systems with Fujitsu FX1 as Core Computer." *Fujitsu Sci. Tech. J* 44.4 (2008): 426-434.